Acta Geologica Sinica (English Edition), 2020, 94(3): 822–830

# Rapid Determination of Complete Distribution of Pore and Throat in Tight Oil Sandstone of Triassic Yanchang Formation in Ordos Basin, China

DU Shuheng[1, *] and SHI Yongmin[2]

[1] *State Key Laboratory of Nonlinear Mechanics, Institute of Mechanics, Chinese Academy of Sciences, Beijing 100190, China*
[2] *Oil and Gas Institute, Peking University, Beijing 100871, China*

**Abstract:** This study aimed to investigate the complete distribution of reservoir space in tight oil sandstone combining casting slices, field emission scanning electron microscopy (FE-SEM), the pore-throat theory model, high-resolution image processing, mathematical statistics, and other technical means. Results of reservoir samples from the Xin'anbian area of Ordos Basin showed that the total pore radius curve of the tight oil sandstone reservoir exhibited a multi-peak distribution, and the peaks appeared to be more focused on the ends of the range. This proved that pores with a radius of 1–50,000 nm provided the most significant storage space for tight oil, indicating that special attention should be paid to this range of the pore size distribution. Meanwhile, the complete throat radius curve of the tight oil sandstone reservoir exhibited a multi-peak distribution. However, the peak values were distributed throughout the scales. This confirmed that the throat radius in the tight oil sandstone reservoir was not only in the range of hundreds of nanometers but was also widely distributed in the scale approximately equal to the pore size. The new rapid determination method could provide a precise theoretical basis for the comprehensive evaluation, exploration, and development of a tight oil sandstone reservoir.

**Key words:** complete distribution, tight oil reservoir, multi-precision imaging, mathematical statistics

Citation: Du and Shi, 2020. Rapid Determination of Complete Distribution of Pore and Throat in Tight Oil Sandstone of Triassic Yanchang Formation in Ordos Basin, China. Acta Geologica Sinica (English Edition), 94(3): 822–830. DOI: 10.1111/1755-6724.13881

## 1 Introduction

With the large-scale discovery and industrial exploitation of unconventional oil and gas resources, theoretical research on unconventional reservoirs has become the top priority in oil and gas exploration and development (Jiang et al., 2017; Sima et al., 2017; Jiao, 2019; Du, 2020; Du et al., 2020; Zhang et al., 2020). The core of reservoir research lies in the reservoir space, which mainly consists of pores and fractures. Therefore, many scholars have studied the development characteristics and mechanism of pore, natural fracture and hydraulic fracture in unconventional reservoirs, which has contributed to improving the recovery of resources (Ge et al., 2015a, 2015b; Dai et al., 2017, 2019; Shen and Zhao, 2018; Wang et al., 2018). According to morphological characteristics, pore can be furtherly divided into pore and throat. Meanwhile, fracture is an important part of reservoir space. A high degree of fracture development (found in imaging observation) will play an important role in oil and gas reservoir and seepage. Thus, it is also an important factor to be considered. The pore-throat characteristics and development rule will directly control the reservoir permeability. According to these principles, many productive studies have been conducted based on cast slices, field emission scanning electron microscopy (FE-SEM), high-pressure mercury injection, mercury injection in constant pressure (MICP), nuclear magnetic resonance (NMR), computed tomography scanning, and gas adsorption. These findings have increased our understanding of the reservoir space on different scales and provided a solid foundation for scholars in various fields to understand pore-throat development in different degrees (Du et al., 2018a, 2018b). However, due to the differences in testing principles and accuracy of the technologies examined, the conclusions of various testing methods present certain discrepancies and deviations (Nishank et al., 2017a, 2017b).

Reservoir space development should be investigated in a continuous manner using different scales. Regrettably, current test technologies focus on certain aspects of the reservoir while selectively ignoring other characteristics. Such a limited scope of testing only selected principles of the actual reservoir does not incorporate a global perspective and will thus inevitably generate a faulty conclusion. Based on this observation, some scholars have invested in the construction analysis of the complete pore and throat radius distribution to summarize and evaluate the reservoir space in an inclusive manner and therefore achieve a complete overall conclusion. Kate and Gokhale (2006) introduced a new index to improve the water vapor adsorption method, and constructed complete pore distribution curve of the reservoir rock. Adnan et al.

* Corresponding author. E-mail: dushuheng@imech.ac.cn

(2014) explored the complete pore size distribution range of shale gas reservoir by combining high-pressure mercury injection, nitrogen adsorption and nuclear magnetic resonance, they also claimed that this method could overcome the limitation of individual method. Xiao et al. (2016) established the complete pore radius distribution by combining nuclear magnetic resonance (NMR) spectroscopy and constant-speed mercury injection technology to discover the seepage contribution of a reservoir space with different pore sizes. However, these construction methods exhibit the following critical problems in practical operation.

(1) Although high-pressure mercury injection and nitrogen adsorption are both effective methods for measuring reservoir space, the principles, operation, and precision of these methods are entirely different. It is questionable whether the mechanical splicing of the results of different technologies is logical.

(2) From the perspective of research on reservoirs and permeability, the distinction or segmentation between the pore and the throat appears to be of great significance. However, due to the limited technical principles of high-pressure mercury injection and gas adsorption, these two technologies are unable to distinguish between the pore and the throat. Constant-speed mercury injection is the only fluid experiment that can distinguish between the pore and the throat. However, due to the limitation of the instrument pressure (approximately 6.2 MPa), some pores and throats are selectively ignored. Consequently, the overall appearance of the reservoir is not reflected. Therefore, it is currently impossible to distinguish between the pore and the throat at any scale of the reservoir, although this is the essential aspect of reservoir exploration and development (Shah et al., 2016; Rikan et al., 2017).

Given the limited research on effective methods of thoroughly assessing the pore and throat radius distribution of tight oil sandstone reservoirs, this paper focused on the integration of tight oil exploration and development. In this paper, data from casting slices, FE-SEM imaging, the pore-throat theory model, high-resolution image processing, mathematical statistics, and other technical means were combined. A new method is proposed to provide the complete pore and throat radius distribution in a tight oil sandstone reservoir ranging from 0 nm to 180,000 nm. This approach cleverly avoids the logical confusion sourced from splicing the test data of different technologies by performing pore and throat segmentation and characterization of the reservoir space on any scale and subsequently characterizing them separately. This tactic provides a highly precise theoretical basis for the comprehensive evaluation, exploration, and development of a tight oil sandstone reservoir.

## 2 Geologic Settings

Ordos Basin, which is in the west of the north China block, is a large multi-cycle craton basin with the occurrence of whole lift and depression migration (Zhang et al., 1997; Liu, 1998; Su et al., 2003; Xiao et al., 2005; Yuan et al., 2007) (Fig. 1).

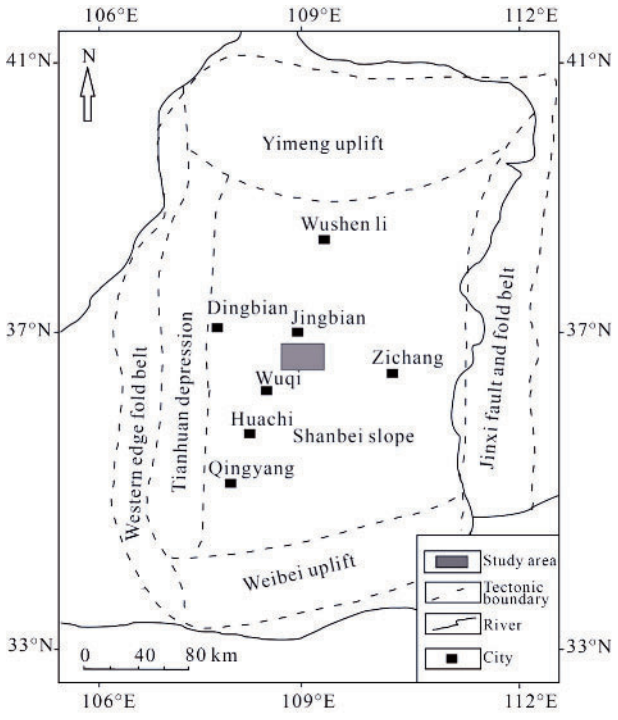


Fig. 1. Location of the study area in Ordos Basin, China (Revised after Du et al., 2019).

Based on the tectonic development history of the basins, sedimentation, and the superface structure of the Ordovician strata, the Paleozoic structure in Ordos Basin can be classified into six tectonic units, namely, Western edge fault belt, Tianhuan depression, Shanbei slope, Jinxi fault and fold belt, Weibei uplift, and Yimeng uplift. The structure inside the basin is relatively simple. Abundant oil resources exist in the ultra-low permeability Upper Triassic Yanchang Formation, which is part of a lake-delta sedimentary system (Zhang et al., 1997; Liu, 1998; Darby and Ritts, 2002; Su et al., 2003; Gan et al., 2007).

In terms of the stratigraphy and depositional facies, Yanchang Formation, as the main hydrocarbon reservoir, is characterized by deposits from the lake delta front and delta plain with a large area. The correlation between oil-bearing and physical properties is strong. The distribution range of the sand body controls the distribution range of the reservoirs, and this process is conducive to the formation of large-scale lithologic reservoirs (Zhang et al., 1998; Bradley et al., 2004; Cai et al., 2005; Ji and Meng, 2006; Zhang et al., 2007). The reservoir development of Yanchang Formation is generally regular; sand and mudstone boundaries are generally flat and extensively extended, and it is easy to distinguish a single sand body with a thickness of about 3 m. At the same time, the phenomenon of sand body pinch-out is obvious in some places, and interlayers are widely developed (Li et al., 2011; Du et al., 2018a, 2018b).

Samples of these studies were obtained from wells located in Xin'anbian District, Hujianshan Oilfield, Ordos Basin. The wells are all in the southwestern part of northern Shanbei slope in the basin. Yanchang Formation is derived from clastic rock dominated by lacustrine

sediments in the Late Triassic. As shown in Fig. 2, porosity and permeability of 1500 samples showed that the average porosity is 7.0%, and the permeability is $0.11\times10^{-3}$ μm$^2$. It should be pointed out that the permeability in Fig. 2 is the absolute permeability measured by water. As micro-fractures develop in some reservoir samples, the permeability of these samples could reach about $5\times10^{-3}$ μm$^2$, which is common. The pore types are primarily inter-granular and dissolved pores, and the primary inter-granular, secondary inter-granular, and secondary dissolved pores are relatively developed.

## 3 Methods and Results

### 3.1 Technical route

Based on FE-SEM (maximum accuracy of 0.5 nm) and energy spectrum analysis, this study attempts to return to the geological principle itself and puts forward a new idea of constructing the complete pore and throat radius distribution in a tight oil reservoir. The specific technical route is shown in Fig. 3.

In the first step, the pore types and their content statistics could be identified. In the second step, we could use the watershed and other algorithms to extract the pore-throat and conduct pore-throat segmentation. In the third step, we calculated the pore-throat parameters and the cumulative probability in each single view. In the last step, the total pore and throat radius curve could be constructed.

It should be pointed out that in this paper, after the complete pore and throat distribution curve of the reservoir was constructed, 143 samples were selected. Each sample must be observed 1000 views to ensure that all the information could be used in the research. Finally, in order to ensure accuracy of the calculation results, large -scale mathematical calculations were effectively completed with the use of a computer.

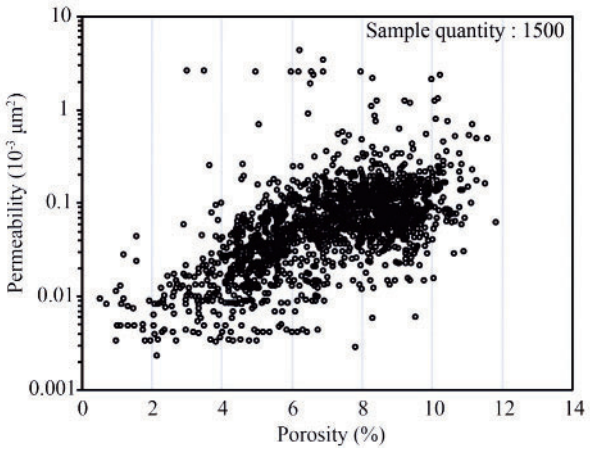


Fig. 2. Porosity and permeability of the samples from Yanchang Formation, Xin'anbian District, Ordos Basin.

### 3.2 Thin section observations

Observations of cast thin film sections (Fig. 4) demonstrated that the overall development of the reservoir pores in the tight sandstone in the Xin'anbian area of Ordos Basin is low. The main pore types are inter-granular and feldspar dissolution pores, and the primary throat types are contractive-neck and bent-sheet. The pore and throat distributions affect the permeability and production capacity of the reservoir.

### 3.3 High-precision FE-SEM imaging

As shown in Fig. 5, the FE-SEM data demonstrated that the inter-granular and feldspar dissolution pores are widely developed, including dissolution pores of debris and inter-crystalline pores, such as inter-granular pores in kaolinite. The dissolution pores of debris and inter-crystalline pores are far smaller than macropores, such as inter-granular pores, but the dissolution pores of debris and inter-crystalline pores have larger surface areas.

Therefore, they provide available space for tight oil storage and seepage. However, due to technological limitations, our current approach could only test the nanopores by gas adsorption. Such test results are rarely combined and compared with those of macropores, so the actual contribution of the nanopores to the tight oil sandstone reservoir is ambiguous. Moreover, the identification of the pore and throat distribution is significant to microscale seepage. Therefore, the construction of the complete pore and throat radius is particularly essential.

The distribution histogram of the four pore types was obtained from an observation of 200 thin slices of tight sandstone samples. Fig. 6 illustrates that inter-granular and feldspar dissolution pores are the primary pore types, representing approximately 48% and 47%, respectively, of all pore types. The dissolution pores of debris and inter-crystalline pores account for 3% and 2%, respectively, of the total. The content of the dissolution pores of debris and inter-crystalline pores is relatively small in comparison with those of the inter-granular and inner-feldspar dissolution pores, and the crude oil in these pores is difficult to exploit. Most of the oil located in the dissolution pores of debris and inter-crystalline pores is residual oil, and exploitation is also quite challenging. Further technological breakthroughs and mechanism studies are needed.

### 3.4 Cumulative probability distribution of the pore and throat distributions

Tight oil sandstone reservoir samples in the Xin'anbian area of Ordos Basin were selected. Single pore and throat parameter calculations were conducted, and a cumulative

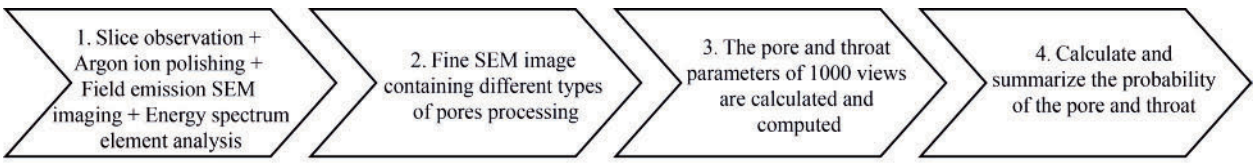


Fig. 3. Flowchart of the construction process of the complete pore and throat radius analysis.

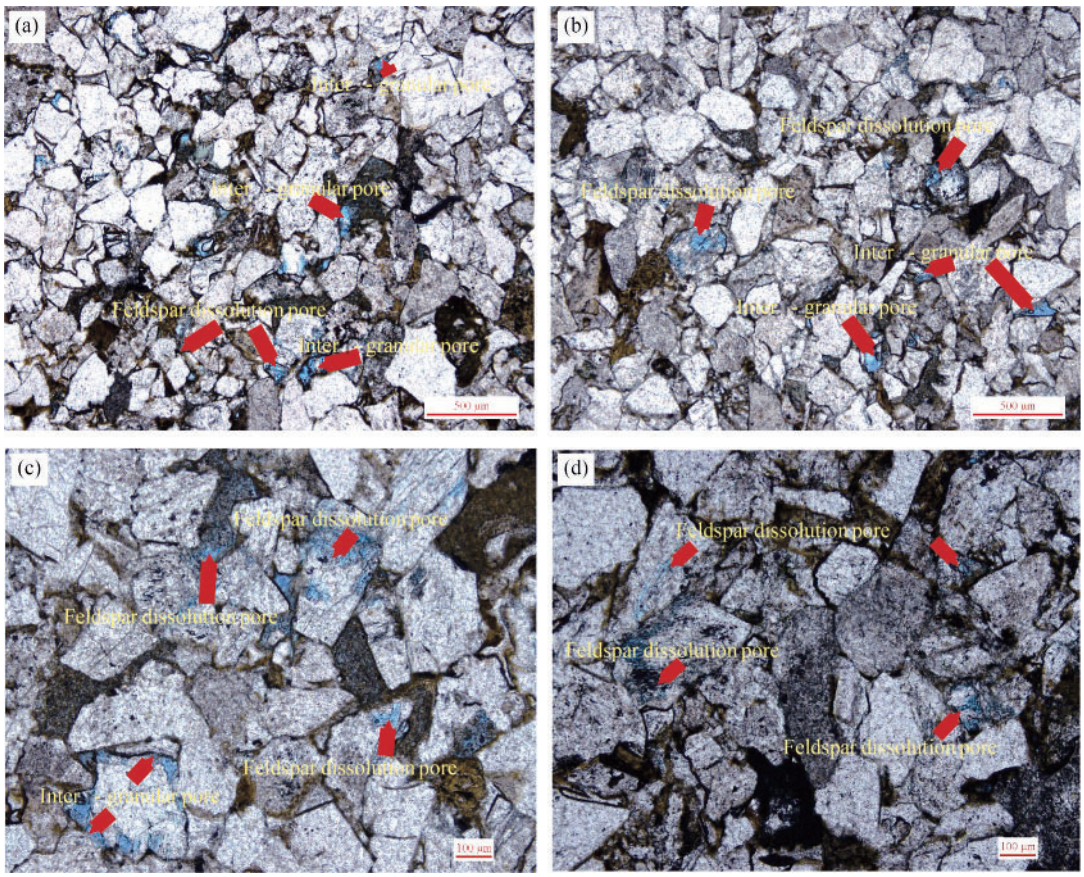


Fig. 4. Observation of the tight oil sandstone reservoir of the Yanchang Formation in Ordos Basin, China based on thin-section casting.
(a) Well A1, Yanchang Formation, sampling depth of 2173.5 m; (b) Well A2, Yanchang Formation, sampling depth of 2159.3 m; (c) Well A3, Yanchang Formation, sampling depth of 2184.9 m; (d) Well A4, Yanchang Formation, sampling depth of 2259.76 m.

probability curve was prepared based on images with different resolutions and scales. The ratio between the frequency of each pore and throat radius in a single image and the image area was calculated to yield the pore and throat frequency in the unit area. Finally, the probability of all the frequencies and the complete pore and throat distribution curve construction were summarized.

## 4 Discussion

### 4.1 Advantages and disadvantages of testing in a tight oil reservoir

Most research on the pore and throat characteristics of reservoirs depends on the development of various testing techniques. The technology of cast thin film sections could determine the development of a reservoir space based on the distribution of the dyeing resin fluid in the reservoir. Although some technical details are available about casting image processing in the petroleum and natural gas industry of China, limitations such as low precision, poor image quality, and fabrication difficulties cannot be ignored. Therefore, the image of a cast thin film section may be suitable for the qualitative observation of a reservoir space but not for generating quantitative conclusions in a tight oil sandstone reservoir.

High-pressure mercury injection is a fast and effective method primarily based on the Laplace equation (capillary force formula). In this process, the pressure change of the mercury injection is used to study the degree of development of the pore and throat in a reservoir. The constant velocity of the mercury pressure is based on the pressure rise and fall of the low-pressure mercury injection process, and it elucidates the separation of the pore and throat for studying the seepage capacity of the reservoir. However, these two methods selectively ignore the presence of some pore and throat distributions due to the randomness of the seepage process. Because of the difference between the properties of mercury and geological fluids, the optimization of results needs further exploration.

In NMR technology, the fluid relaxation time corresponds to the reservoir space with relative scale, and it is an advanced and effective way to identify the reservoir space efficiently. However, even with the present developments in this technology, no new progress has been made in distinguishing pores and throats.

Micro- or nano-CT scanning has been widely used in the characterization of unconventional reservoir spaces in recent years, and its importance and superiority are self-evident. Silin et al. and others proposed the maximum sphere method (Silin et al., 2003; Dong, 2007), which segments pores and throats based on CT data. Like other technologies, this approach has shortcomings. For example, the resolution and representativeness cannot be

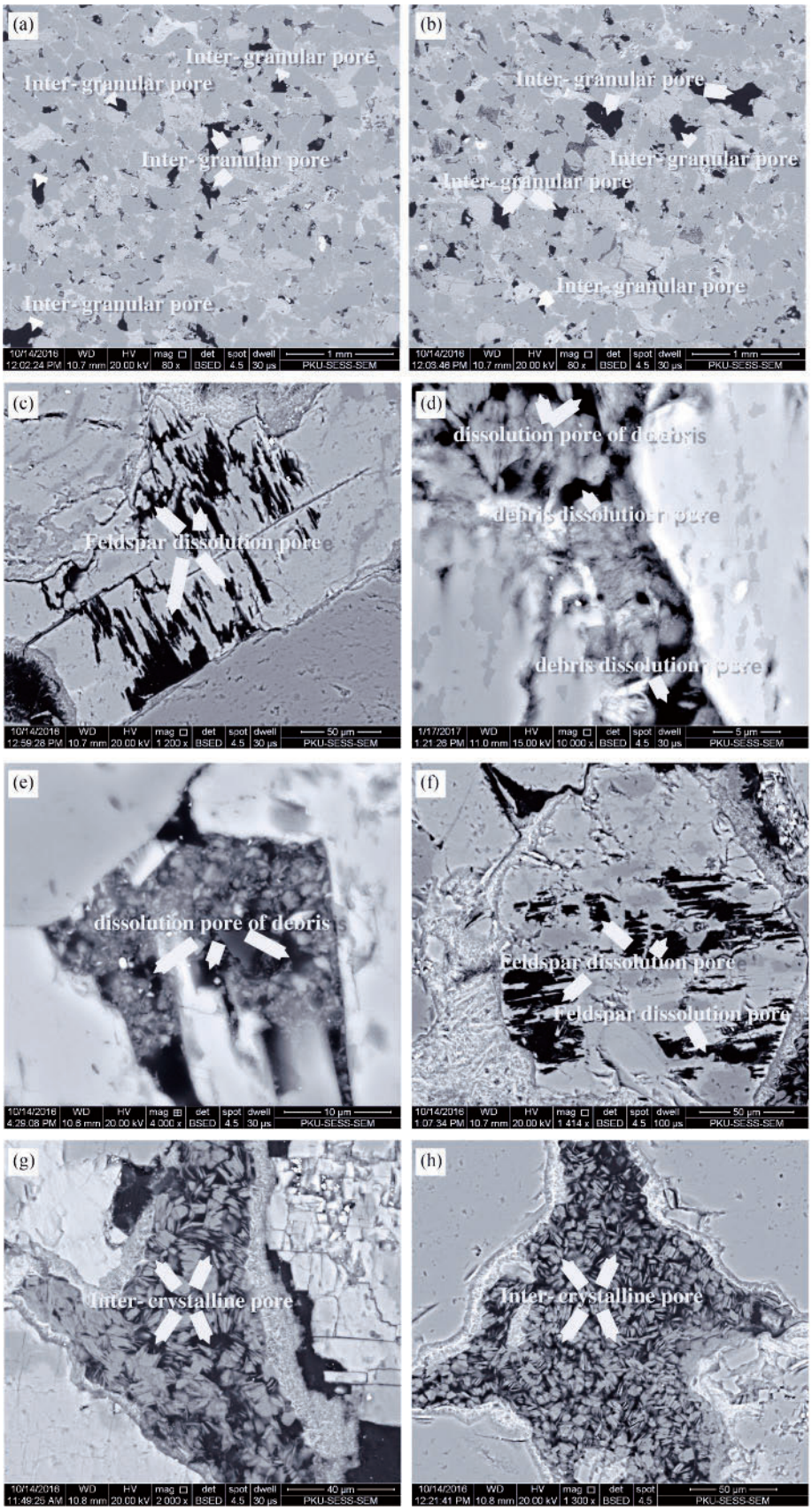


Fig. 5. FE-SEM observation of the tight oil sandstone reservoir of Yanchang Formation in Ordos Basin, China.
(a, b) Well H198, Yanchang Formation, sampling depth of 2173.5 m; (c, d) Well, A237-40, Yanchang Formation, sampling depth of 2159.3 m; (e) Well H191, Yanchang Formation, sampling depth of 2184.9 m; (f) Well A238-27, Yanchang Formation, sampling depth of 2259.76 m; (g) Well A83, Yanchang Formation, sampling depth of 2190.5 m; (h) Well A238-27, Yanchang Formation, sampling depth of 2275.5 m.

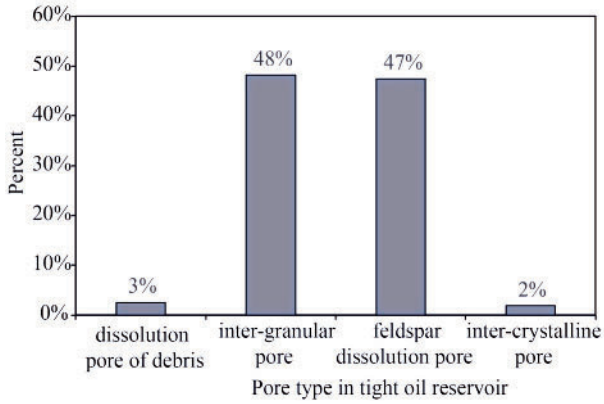


Fig. 6. Distribution histogram of pore type division in the tight oil reservoir.

assessed simultaneously, and the types of pores and throats cannot be judged.

Gas adsorption has a unique advantage in measuring ultra-micropores in the range of 1–100 nm because the molecular radius of gas is very small. However, this method is unable to distinguish between pores and throats and hence was not used in this study.

FE-SEM imaging could be effective in studies of tight oil sandstone reservoirs based on the conductivity of minerals. Accurate to 0.5 nm, FE-SEM can be used to identify pore and throat space effectively, and its accuracy is greater than that of casting thin sections. Additionally, it is nondestructive to the reservoir sample. The observation range in FE-SEM is larger than the sample size and analysis scale of nano-CT, and its ease of operation and low cost are somewhat better than those of NMR. Therefore, to accurately identify the pore and the throat, this study will identify the pore-throat distribution and evaluate the related minerals lining the pore-throat regions effectively by combining FE-SEM with energy spectrum analysis.

Newer reservoir testing technologies, such as CT and focused ion beam-scanning electron microscopy (FIB-SEM), have been introduced. However, the original technologies for reservoir characterization based on two-dimensional characterization methods and techniques still provide important information. That is, sufficient focus on the research purpose, continuous exploration of existing mature technology, and acquisition of new information can also be regarded as the best use of everything and information fusion.

For assessment of both reservoir and development geology, reservoir characterization should focus on improving oil recovery and clarifying the occurrence position and flow mechanism of oil and gas. Therefore, 2D data should be studied entirely. Evaluation of 2D data still has considerable potential in research for (1) solving the contradiction between representation and resolution in a short time and applying to crucial technologies, such as high precision scanning, storage, statistics, and analysis of massive reservoir data and (2) improving CT resolution and scanning scale. Therefore, attention to the 2D information should not be reduced. Furthermore, with the development of wide-field imaging technology, the contradiction between the resolution and representation is first resolved in the 2D space. The concept of pore and throat distributions and the discovery of ultra-nanopores in shale gas reservoirs are both based on the observation and characterization of cast thin film sections or FE-SEM in the 2D space. The standard in the oil and gas industry also consists of pore-throat image analysis in 2D.

### 4.2 Application of new method

With reservoir samples from the Xin'anbian area of Ordos Basin as example, 300 images of the reservoir were selected according to the percentage of porosity development. The entire pore and throat distribution curves were prepared.

As can be seen from Figure 7, the nanopores and throats occupy more than 90% of the total number of pore and throat features in the tight oil reservoirs, which are mostly concentrated in the range of 29.12–37.37 nm. Due to the small volume of the nanopore space itself, the reservoir capacity is weaker than for macropores, but the nanopores cannot be ignored because of their large number.

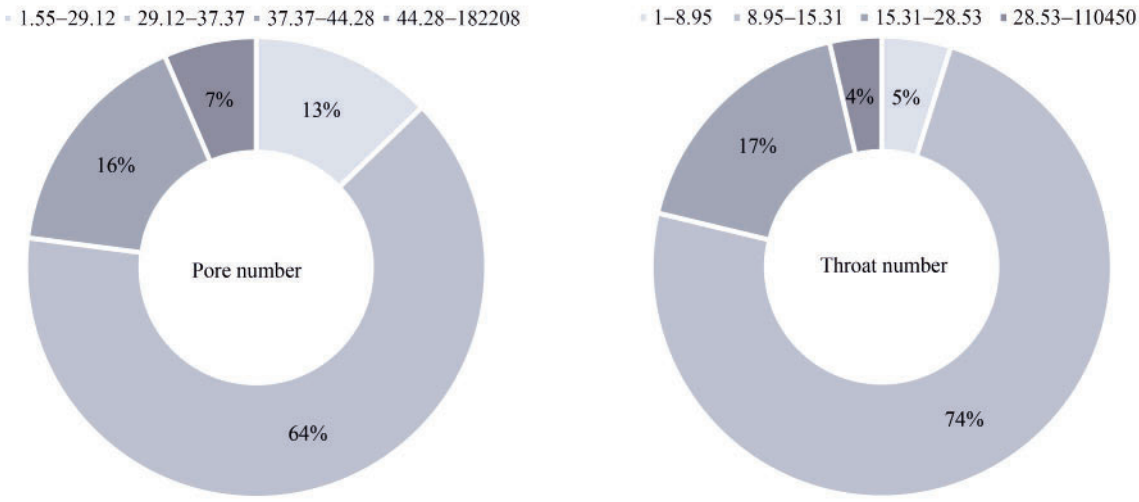


Fig. 7. Number distribution of pores (1.55–182,208 nm) and throats (0.47–110,450 nm) in different images with the relative scales.

Figure 8 and Figure 9 represent the distribution curve and cumulative probability curve of the complete pore and throat radius distributions, respectively, of the reservoir samples of the tight oil sandstone reservoir in the Xin'anbian area of Ordos Basin. Figure 8 shows that the total pore radius curve of the tight oil sandstone reservoir exhibited a multi-peak distribution, and the peaks appear more focused on the ends of the range.

Pore radius less than 500 nm accounted for approximately 10% (nanopores), 500–2,000 nm accounted for 15% (micropores), 2,000–10,000 nm accounted for approximately 27% (small pores), 10,000–20,000 nm accounted for approximately 13% (middle pore), and greater than 20,000 nm accounted for approximately 25% (large pore) of the pore radius distribution. The minimum pore radius was 1.55 nm, the median pore radius (the value when the cumulative content reached 50%) was 7,780 nm, and the maximum pore radius was 182,210 nm.

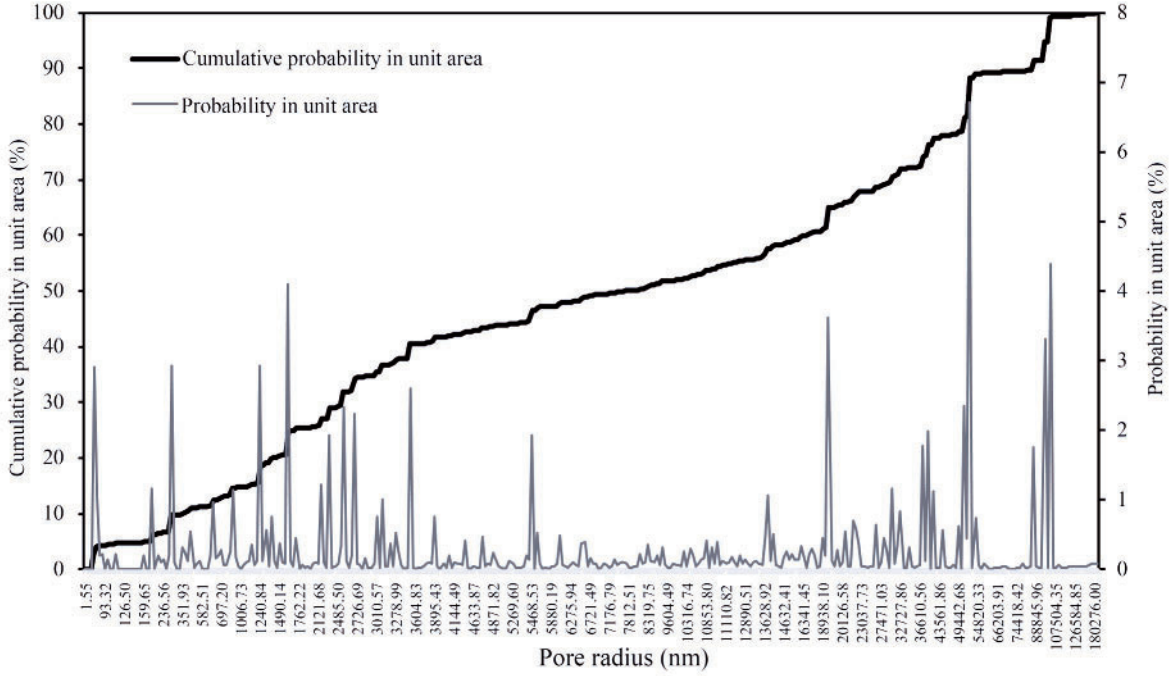


Fig. 8. Complete pore radius distribution and the cumulative probability of reservoir samples of the tight oil sandstone reservoir in the Xin'anbian area of Ordos Basin.

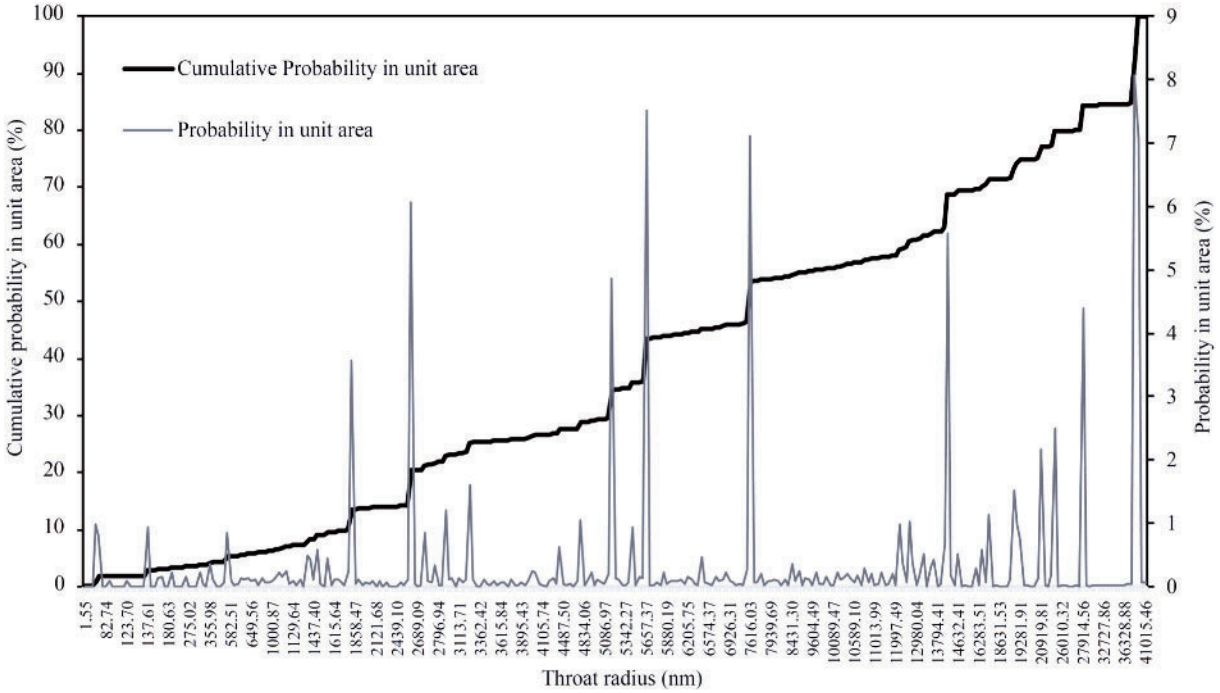


Fig. 9. Complete throat radius distribution and the cumulative probability of reservoir samples of the tight oil sandstone reservoir in the Xin'anbian area of Ordos Basin.

The data indicated that the occurrence of tight oil is not only concentrated in nanoscale pores. Pores with a radius of 1–50,000 nm provide the most significant storage space for tight oil, indicating that special attention should be paid to this range of the pore size distribution. Evaluation of the distribution curve and cumulative probability curve of the complete pore radius distribution can increase knowledge of pores, which are partially neglected in testing by the high-pressure mercury and constant-speed mercury injection techniques. This application is a useful complement to the other three-dimensional testing technologies.

Similarly, Figure 9 illustrates that the complete throat radius curve of the tight oil sandstone reservoir exhibited a multi-peak distribution; however, the peak values are distributed throughout the scales. Throat radius less than 500 nm accounts for approximately 5% (nanothroat), 500–2,000 nm for 9.5% (micro throat), 2,000–10,000 nm for 43.5% (small throat), 10,000–20,000 nm for 20% (middle throat), and greater than 20,000 nm for 22% (large throat) of the throat radius distribution. The minimum value determined for the throat radius was 0.47 nm, the median throat radius (the value when the cumulative content reached 50%) was 6,730 nm, and the maximum throat radius was 110,450 nm. The data demonstrated that the throat radius in the tight oil sandstone reservoir is not only in the range of hundreds of nanometers but is also widely distributed in the scale approximately equal to the pore size.

Many factors make exploitation of the tight oil sandstone reservoir difficult. Not only the narrow throat radius but also the substantial quantity of specific surface area in clay minerals, which could provide a larger facade for residual oil adsorption, could influence exploitation of the tight oil sandstone reservoir. Even reduced exploitation of crude oil in the narrow throat distributions will result in greater resistance to fluid flow, which should be considered.

## 5 Conclusions

The distributions of the inter-granular and feldspar dissolution pores, which are the primary pore types, are approximately 48% and 47% , respectively. The dissolution pores of debris and the inter-crystalline pores occupy 3% and 2%, respectively. The content of the dissolution pores of debris and the inter-crystalline pores is relatively small in comparison with those of the inter-granular and inner-feldspar dissolution pores, and crude oil is difficult to exploit in these pores. Most of the oil located in the dissolution pores of debris and the inter-crystalline pores is residual oil, which is difficult to exploit. Further technological breakthroughs and mechanism studies are needed.

The nanopores and nanothroats account for more than 90% of the total distribution of the pores and throats in the tight oil reservoirs, occurring primarily in the range of 29.12–37.37 nm. Due to the small volume of the nanopore space itself, the reservoir capacity is weaker than for macropores, but the nanopores cannot be ignored because of their large quantities.

The distribution curve and the cumulative probability curve of the complete inventory of the pore and throat radius features proposed in this study potentially enlarge the number of pores, which are partially neglected in tests involving high-pressure mercury and constant-speed mercury injection. The approach developed is a useful complement to other three-dimensional testing technologies that could be used in unconventional reservoirs, such as tight sandstone, shale, volcanic rock, oil shale, oil sand, and gas hydrate.

## Acknowledgments

This work was jointly supported by National Natural Science Foundation of China (Grant No. 41902132, 11872363, 51861145314), PetroChina Innovation Foundation (Grant No. 2019D-5007-0214), Chinese Academy of Sciences (CAS) through the CAS Key Research Program of Frontier Sciences (Grant No. QYZDJ-SSW-JSC019) the CAS Strategic Priority Research Program (Grant No. XDB22040401) and National Science and Technology Mega Project of China (Grant No. 2017ZX05013005-009).

Manuscript received Nov. 03, 2018
accepted Mar. 15, 2019
associate EIC: HAO Ziguo
edited by HUANG Daomao

## References

Adnan, A.H., Reza, R., Lionel, E., and Labani, M., 2014. Comparisons of pore size distribution: A case from the Western Australian gas shale formations. Journal of Unconventional Oil and Gas Resources, 8: 1–13.

Bradley, D.R., Andrew, D.H., Brian, J.D., Lynde, N., and Adrian, B., 2004. Sedimentary record of Triassic intraplate extension in North China: Evidence from the nonmarine NW Ordos Basin, Helan Shan and Zhuozi Shan. Tectonophysics, 386(3–4): 177–202.

Cai, C.F., Hu, G.Y., He, H., Li, J., Li, J.F., and Wu, Y.S., 2005. Geochemical characteristics and origin of natural gas and thermochemical sulphate reduction in Ordovician carbonates in the Ordos Basin, China. Journal of Petroleum Science and Engineering, 48(3–4): 209–226.

Dai, C., Liu, H., Wang, Y.N., Li, X., and Wang, W.H., 2019. A simulation approach for shale gas development in China with embedded discrete fracture modeling. Marine and Petroleum Geology, 100: 519–529.

Dai, C., Xue, L., Wang, W.H., and Li, X., 2017. Analysis of the influencing factors on the well performance in shale gas reservoir. Geofluids, 2017: 1–12.

Darby, B.J., and Ritts, B.D., 2002, Mesozoic contractional deformation in the middle of the Asian tectonic collage: The intraplate Western Ordos Fold Thrust Belt, China. Earth and Planetary Science Letters, 205: 13–24.

Dong, H., 2007. Micro‐CT imaging and pore network extraction. London: Imperial College, 43–51.

Du, S.H., Pang, S., and Shi, Y.M., 2018a. A new and more precise experiment method for characterizing the mineralogical heterogeneity of unconventional hydrocarbon reservoirs. Fuel, 232: 666–671.

Du, S.H., Pang, S., and Shi, Y.M., 2018b. Quantitative characterization on the microscopic pore heterogeneity of tight oil sandstone reservoir by considering both the resolution and representativeness. Journal of Petroleum Science and Engineering, 169: 388–392.

Du, S.H., Shi, G.X., Yue, X.J., Kou, G., Zhou, B., and Shi, Y.M., 2019. Imaging-Based Characterization of Perthite in the

Upper Triassic Yanchang Formation Tight Sandstone of the Ordos Basin, China. Acta Geologica Sinica (English edition), 93(2): 373–385.

Du, S.H., Shi, Y.M., Zheng, X.J., and Chai, G.S., 2020. Using "Umbrella Deconstruction & Energy Dispersive Spectrometer (UD-EDS)" technique to quantify the anisotropic elements distribution of" Chang 7" shale and its significance. Energy, 191: 116443.

Du, S.H., 2020. Characteristics and the formation mechanism of the heterogeneous microfractures in the tight oil reservoir of Ordos Basin, China. Journal of Petroleum Science and Engineering, 191: 107176.

Gan, H.J., Xiao, X.M., Lu, Y.C., Jin, Y.B., Tian, H., and Liu, D.H., 2007. Genetic relationship between natural gas dispersal zone and uranium accumulation in the northern Ordos Basin, China. Acta Geologica Sinica (English edition), 81: 501–509.

Ge, X.M., Fan, Y.R., Li, J.T., and Muhammad, A.Z., 2015a. Pore structure characterization and classification using multifractal theory—An application in Santanghu basin of Western China. Journal of Petroleum Science and Engineering, 127: 297–304.

Ge, X.M., Fan, Y.R., Zhu, X.J., and Chen, Y.G., 2015b. Determination of nuclear magnetic resonance $T_2$ cutoff value based on multifractal theory—An application in sandstone with complex pore structure. Geophysics, 80(1): D11–D21.

Ji, L.M., and Meng, F.W., 2006. Palynology of Yanchang Formation of middle and late Triassic in eastern Gansu Province and its paleoclimatic Significance. Journal of China University of Geosciences,17(3): 209–220 (in Chinese with English abstract).

Jiang, T.W., Teng, X.Q., and Yang, X.T., 2017. Integrated techniques for rapid and highly-efficient development and production of ultra-deep tight sand gas reservoirs of Keshen 8 Block in the Tarim Basin. Natural Gas Industry B, 4(1): 30–38.

Jiao, F.Z., 2019. Theoretical insights, core technologies and practices concerning "volume development" of shale gas in China. Natural Gas Industry B, 6(6): 525–538.

Kate, J.M., and Gokhale, C.S., 2006. A simple method to estimate complete pore size distribution of rocks. Engineering Geology, 84(1–2): 48–69.

Li, X.B., Chen, Q.L., Liu, H.Q., Wan, Y.R., Wei, L.H., Liao, J.B., and Long, L.W., 2011. Features of sandy debris flows of the Yanchang Formation in the Ordos Basin and its oil and gas exploration significance. Acta Geologica Sinica (English edition), 85: 1187–1202.

Liu, S.F., 1998. The coupling mechanism of basin and orogen in the western Ordos Basin and adjacent regions of China. Journal of Asian Earth Sciences, 16(4): 369–383.

Nishank, S., Ronny, H., and Faruk, O.A., 2017a. Effect of image segmentation & voxel size on micro-CT computed effective transport & elastic properties. Marine and Petroleum Geology, 86: 972–990.

Nishank, S., Ronny, H., and Faruk, O.A., 2017b. References and benchmarks for pore-scale flow simulated using micro-CT images of porous media and digital rocks. Advances in Water Resources, 109: 211–235.

Rikan, K., Pablo, C., Jon, G., Leon, B., Stephen, H., and Greenwell, H.C., 2017. Multi-technique approach to the petrophysical characterization of Berea sandstone core plugs (Cleveland Quarries, USA). Journal of Petroleum Science and Engineering, 149: 436–455.

Shah, S.M., Gray, F., Crawshaw, J.P., and Boek, E.S., 2016. Micro-computed tomography pore-scale study of flow in porous media: Effect of voxel resolution. Advances in Water Resources, 95: 276–287.

Shen, W.H., and Zhao, Y.P., 2018. Combined effect of pressure and shear stress on penny-shaped fluid-driven cracks. ASME Journal of Applied Mechanics, 85(3): 031003.

Silin, D.B., Jin, G.D., and Tad, W.P., 2003. Robust determination of the pore space morphology in sedimentary rocks. SPE 84296.

Sima, L.Q., Wang, C., Wang, L., Wu, F., Ma, L., and Wang, Z.J., 2017. Effect of pore structure on the seepage characteristics of tight sandstone reservoirs: A case study of Upper Jurassic Penglaizhen Fm reservoirs in the western Sichuan Basin. Natural Gas Industry B, 4(1): 17–24.

Su, X.B., Zhang, L.P., and Zhang, R.L., 2003. The abnormal pressure regime of the Pennsylvanian No. 8 coalbed methane reservoir in Liulin–Wupu District, Eastern Ordos Basin, China. International Journal of Coal Geology, 53(4): 227–239.

Wang, L., Dai, C., and Xue, L., 2018. A semianalytical model for pumping tests in finite heterogeneous confined aquifers with arbitrarily shaped boundary. Water Resources Research, 54(4): 3207–3216.

Xiao, D.S., Lu, S.F., and Lu, Z.Y., 2016. Combining nuclear magnetic resonance and rate-controlled porosimetry to probe the pore-throat structure of tight sandstones. Petroleum Exploration and Development, 6: 961–970.

Xiao, X.M., Zhao, B.Q., Thu, Z.L., Song, Z.G., and Wilkins, R.W.T., 2005. Upper Paleozoic petroleum system, Ordos Basin, China. Marine and Petroleum Geology, 22(8): 945–963.

Yuan, Y.S., Hu, S.B., Wang, H.J., and Sun, F.J., 2007. Meso-Cenozoic tectonothermal evolution of Ordos basin, central China: Insights from newly acquired vitrinite reflectance data and a revision of existing paleothermal indicator data. Journal of Geodynamics, 44(1–2): 33–46.

Zhang, L.H., Liu, X.Y., Zhao, Y.L., Zhou, Y., and Shan, B., 2020. Effect of pore throat structure on micro-scale seepage characteristics of tight gas reservoirs. Natural Gas Industry B, 7(2): 160–167.

Zhang, Y.Q., Liao, C.Z., Shi, W., Zhang, T., and Guo, F.G., 2007. Jurassic deformation in and around the Ordos Basin, North China. Earth Science Frontiers, 14(2): 182–196 (in Chinese with English abstract).

Zhang, L.F., Sun, M., Wang, S.G., and Yu, X.Y., 1998. The composition of shales from the Ordos Basin, China: Effects of source weathering and diagenesis. Sedimentary Geology, 116 (1–2): 129–141.

Zhang, Z.L., Sun, K.Q., and Yin, J.R., 1997. Sedimentology and sequence stratigraphy of the Shanxi Formation (Lower Permian) in the northwestern Ordos Basin, China: An alternative sequence model for fluvial strata. Sedimentary Geology, 112(1–2): 123–136.

## About the first and corresponding author

DU Shuheng, male, born in 1994 in Dingyuan County, Anhui Province; doctor; graduated from Peking University; assistant professor of State Key Laboratory of Nonlinear Mechanics, Institute of Mechanics, Chinese Academy of Sciences. He is now interested in the study on unconventional hydrocarbon geology and mechanics. Email: dushuheng@imech.ac.cn; phone: 010-82543677, 18813134652.